Improved Genetic Optimization Algorithm with Subdomain Model for Multi-objective Optimal Design of SPMSM

Jian Gao, Litao Dai and Wenjuan Zhang

***Abstract*—For an optimal design of a surface-mounted permanent magnet synchronous motor (SPMSM), many objective functions should be considered. The classical optimization methods, which have been habitually designed based on magnetic circuit law or finite element analysis (FEA), have inaccuracy or calculation time problems when solving the multi-objective problems. To address these problems, the multi-independent -population genetic algorithm (MGA) combined with subdomain (SD) model are proposed to improve the performance of SPMSM such as magnetic field distribution, cost and efficiency. In order to analyze the flux density harmonics accurately, the accurate SD model is first established. Then, the MGA with time-saving SD model are employed to search for solutions which belong to the Pareto optimal set. Finally, for the purpose of validation, the electromagnetic performance of the new design motor are investigated by FEA, comparing with the initial design and conventional GA optimal design to demonstrate the advantage of MGA optimization method.**

***Index Terms*—Improved Genetic Algorithm, reduction of flux density spatial distortion, sub-domain model, multi-objective optimal design.**

I. INTRODUCTION

HIGH performance permanent magnet synchronous motors are of high demand in industrial applications like electric vehicle due to the requirements of high efficiency, low cost, low acoustic noise and smooth torque [1-3].

The energy efficiency is strongly associated with electrical motors, a higher efficiency motor consumes less energy than a standard one [4-9]. And the cost of the materials is a nonnegligible part of the PM machines optimal design [10-11]. Due to the spatial harmonics can induce mechanical vibration and acoustic noise, hence the smooth torque is preferable in industrial applications [12-17]. Consequently, efficiency maximization, cost minimization and flux density spatial optimization become the important parts of the PM machines optimal design.

In general, for multi objective optimization problems, the global optimization techniques are required for electric machines. During the past years, particle swarm optimization (PSO) have been used, e.g., in [10] and [12], genetic algorithm (GA) optimization method in [3] and [9]. There are also some new optimization strategies [1] and [2]. In [10], a modified PSO is proposed to search the cost value of the global best during in the current iteration. In [2], an interactive multiobjective optimization method is presented to find the most preferred Pareto optimal solution for six objective functions. Accordingly, the improved intelligent algorithm is more advantageous to solve the multi-objective optimization problem.

Since the simplified model such as equivalent magnetic circuit method cannot describe the relationships between the amplitude of flux density harmonics and the structural parameters of motor [6][14][19]. Numerical methods, such as finite element analysis (FEA) can account for the complicated structure and material saturation. However, numerical methods are combined with optimization will relatively slow and time-consuming [2]. The SD model are fast and can provide reliable predictions of the magnetic field computation in electrical machines as analytical model [16][18].

In this paper, an accurate SD model is presented to analyze the harmonic order of flux density in SPMSM, and the FEA shows excellent accuracy of the analytical solutions. An improved genetic algorithm, as multi- independent-population genetic algorithm (MGA), which based on SD model can solve the multi-objective functions is presented to optimize the performance of the investigated SPMSM, including the operating efficiency, material cost and electromagnetic waveforms.

II. MODELING

A. THD of Air-gap Flux Density

In order to save the computational time of optimal algorithm, a SD model without the effect of slot is established in this paper. The SD model is based on two-dimensional models in polar coordinates and solves the governing Laplacian and quasi-Poissonian field equations in the air gap and magnet

This article was submitted for review on 01, February, 2018.

This work was supported in part by the National Natural Science Foundation of China under Grant51507016.

Jian Gao is with the College of Electrical and Information Engineering, Hunan University, Changsha, 410082 China, (e-mail: Gaojian0895@hnu.edu.cn).

Litao Dai is with the College of Electrical and Information Engineering, Hunan University, Changsha, 410082 China (e-mail: 635757114@qq.com).

Wenjuan Zhang is with the College of Electronic Information and Electrical Engineering, Changsha University, Changsha, 410002 China (e-mail: 441291390@qq.com).

regions.

The following assumptions are made to obtain an analytical solution for the air-gap field distribution produced by permanent magnets. 1) The permanent magnets have a linear demagnetization characteristic. 2) End-effects are neglected. 3) The stator and rotor back-iron is infinitely permeable.

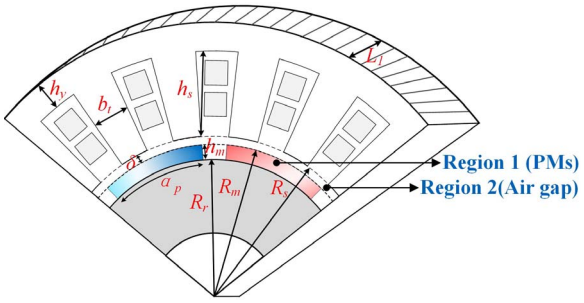

Fig. 1. Surface-mounted PM motor topology.

Fig. 1 shows a simplified view of a SPMSM. The field vectors $\vec{B}$ and $\vec{H}$ in two regions are coupled by

$$\vec{B}_{air} = \mu_0 \vec{H}_{air} \tag{1a}$$

$$\vec{B}_m = \mu_0 \mu_r \vec{H}_m + \mu_0 \vec{M} \tag{1b}$$

where $\vec{B}_{air}$ and $\vec{B}_m$ are the flux density vectors in the air-gap and PMs, respectively, $\vec{H}_{air}$ and $\vec{H}_m$ are the flux intensity vectors in the air-gap and PMs, respectively, μ_0 is the air permeability, μ_r is the relative recoil permeability. For radial magnetization distribution, the magnetization vector $\vec{M}$ can be given as

$$\vec{M} = M_r \vec{r} + M_\theta \vec{\theta} \tag{2}$$

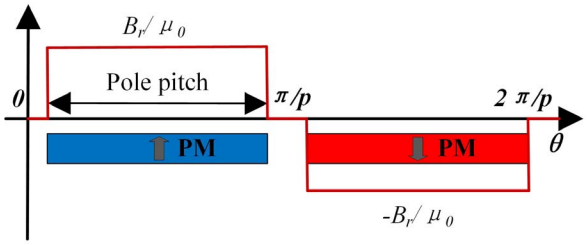

Fig. 2. Waveform of magnetization

Fig. 2 shows the radial magnetization distribution produced by PMs. For radial magnetization, the tangential component M_θ is constant to 0. The radial component can be described, over one pole pair, by

$$\begin{cases} M_r = \dfrac{B_r}{\mu_0} & \dfrac{(1-\alpha_p)\pi}{2p} \le \theta \le \dfrac{(1+\alpha_p)\pi}{2p} \\ M_r = -\dfrac{B_r}{\mu_0} & \dfrac{(3-\alpha_p)\pi}{2p} \le \theta \le \dfrac{(3+\alpha_p)\pi}{2p} \\ M_r = 0 & else \end{cases} \tag{3}$$

where p is the number of pole-pairs, B_r is the remanence, α_p is the magnet pole-arc to pole pitch ratio, and θ is the angular position. M_r can be expressed as Fourier series, i.e.,

$$M_r = \sum_{n=1,3,5,\ldots} \frac{2}{\pi} \left(\frac{\cos\frac{1}{2}[n\pi-(n+1)\alpha_p\pi]}{n+1} + \frac{\cos\frac{1}{2}[n\pi-(n-1)\alpha_p\pi]}{n-1} \right) \tag{4}$$

for n≠1, considering the optimization procedure in this paper.

The scalar magnetic potential φ in the air-gap is governed by Laplacian equation, in the permanent magnet regions it is governed by the quasi-Poissonian equation [18],

$$\frac{\partial^2 \varphi_{air}}{\partial r^2} + \frac{1}{r}\frac{\partial \varphi_{air}}{\partial r} + \frac{1}{r^2}\frac{\partial^2 \varphi_{air}}{\partial \theta^2} = 0 \tag{5a}$$

$$\frac{\partial^2 \varphi_m}{\partial r^2} + \frac{1}{r}\frac{\partial \varphi_m}{\partial r} + \frac{1}{r^2}\frac{\partial^2 \varphi_m}{\partial \theta^2} = \frac{M_r}{\mu_r r}\sin(np\theta) \tag{5b}$$

The boundary conditions are defined by

$$H_{\theta air}(r,\theta)\big|_{r=R_r} = 0 \tag{6a}$$

$$B_{rm}(r,\theta)\big|_{r=R_m} = B_{rair}(r,\theta)\big|_{r=R_m} \tag{6b}$$

$$H_{\theta m}(r,\theta)\big|_{r=R_m} = H_{\theta air}(r,\theta)\big|_{r=R_m} \tag{6c}$$

$$H_{\theta m}(r,\theta)\big|_{r=R_s} = 0 \tag{6d}$$

In the air-gap, general solution to the governing (5) can be obtained as

$$\varphi_{air}(r,\theta) = \sum_{n=1,3,5,\ldots}^{\infty} (A_{nair} r^{np} + B_{nair} r^{-np}) \sin(np\theta) \tag{7}$$

where A_{nair} and B_{nair} are constraints determined by applying continuity conditions (3).

The flux density components are defined by

$$B_r = -\mu \frac{\partial \varphi}{\partial r} \tag{8a}$$

$$B_\theta = -\frac{\mu}{r}\frac{\partial \varphi}{\partial \theta} \tag{8b}$$

The developed analysis model has been validated by FEA on both slotless and slotted motors as shown in Fig. 3 (a) and (b), the result shows that SD model can well predict the amplitude of the air-gap flux density harmonics.

The THD of flux density in air-gap region can be given as

$$THD = \frac{\sqrt{\sum_{i=3,5,7,\ldots} B_i^2}}{B_1} \tag{9}$$

where B_1 and B_i are the harmonic order of air-gap flux density. To save the calculation time, the maximum harmonic number is set to 15 times.

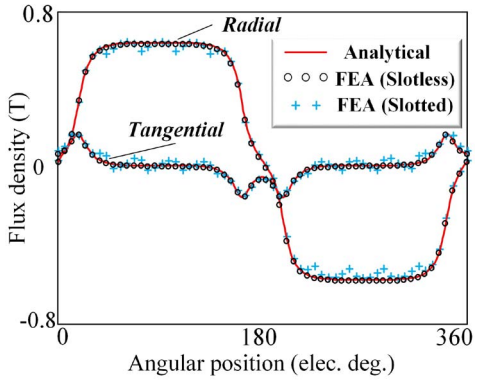

(a)

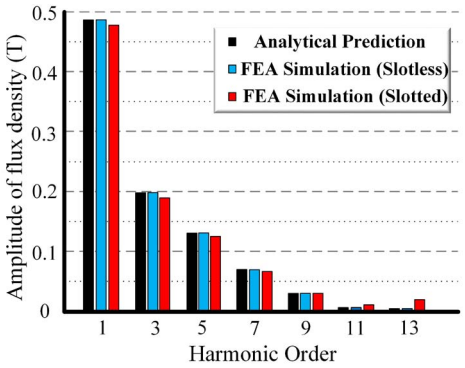

(b)

Fig. 3. A 6-pole 36-slot SPMSM (α_p=0.8) model validation. (a) Air-gap field components with radial magnetized magnets (b) Spatial Fourier decomposition.

B. Cost of SPMSM

For the sake of obtaining the most cost-effective surface-mounted PM motor, the proposed criterion includes the different material cost

$$C_{Act} = c_{Cu}M_{Cu} + c_{Fe}M_{Fe} + c_{PM}M_{PM} \tag{10}$$

where C_{Act} is the active generator material cost, c_{Cu}, c_{Fe}, c_{PM} are the unit costs of the copper, the active iron, and the permanent magnets, and M_{Cu}, M_{Fe}, M_{PM} are the weight of the copper, the active iron, and the permanent magnets, respectively.

C. Efficiency of SPMSM

The most common evaluation of iron loss is the Bertotti iron loss formula [20], which calculates the iron loss per volume as

$$p_{Fe} = k_h B_m^2 f + \frac{\pi^2 \sigma k_d^2}{6} B_m^2 f^2 + k_e B_m^{1.5} f^{1.5} \tag{11}$$

where k_h and k_e are the coefficients of hysteresis loss and excess loss, respectively. σ is the conductivity of the material, and k_d is the thickness of laminations. These four parameters can be referred to the data sheet from steel manufacturer. f is the frequency, and B_m is the peak value of the magnetic flux density.

The average flux density in tooth and yoke can be expressed as [9]

$$B_t = \frac{\pi D_{i1}}{k_s Q_1 b_t} B_g \tag{12a}$$

$$B_y = \frac{D_{i1}}{2k_s p h_y} B_g \tag{12b}$$

where k_s is the stacking factor, D_{i1} is the inner diameter of stator, Q_1 is the number of slots, b_t is the tooth width, and h_y is the yoke height.

The iron loss can be obtained as

$$P_{Fe} = p_{Fet}V_t + p_{Fey}V_y \tag{13}$$

where $V_{t,j}$ are the total volumes of stator tooth and yoke, i.e.,

$$\begin{cases} V_t = h_s b_t L_1 \\ V_y = \pi(D_{i1} + 2h_s + h_y)h_y L_1 \end{cases} \tag{14}$$

and L_1 is the length of core.

The winding resistance can be expressed as

$$R_1 = \rho_{Cu} L_{av} Q_1 / (S_s \cdot S_f) \tag{15}$$

where ρ_{Cu} is the copper electrical resistivity, L_{av} is the length of half winding turn, S_s is the cross-section area of the slot and S_f is the slot filling factor.

The copper losses are given as

$$P_{Cu} = 3I_s^2 R_1 \tag{16}$$

The efficiency η can be calculated as

$$\eta = P_{out} / (P_{Fe} + P_{Cu} + P_{mec} + P_{ad} + P_{out}) \tag{17}$$

where P_{out} is the output power, and the sum of mechanical loss p_{mec} and additional loss p_{ad} are considered as 2% of the rated power.

III. Optimization

In this section, an optimization based on the analytical model is implemented to obtain the optimal geometric structure.

A. Variables and Constraints

A 150-kW SPMSM with a constant speed of 3600 r/min has been chosen to demonstrate the developed analytical model and the optimization method. Table 1 shows the main design details of the PM motor.

The optimization variables have been carefully selected based on the influence of those variables on the optimization process and the quality of the solution, which are independent structural parameters of PM motor. The values of the variables are constrained by the upper and the lower limits, which are set to avoid unacceptable results, eight variables are chosen to vary within a certain range are presented in Table II. The SPMSM structure and design variables are shown in Fig. 1.

The constraints including current density, slot filling factor and the flux density in different regions are as follows:

Subject to:

J_1 (Current density) $\leqslant$ 6 A/mm^2

TABLE I
SPECIFICATIONS OF THE SPMSM

Quantity	Value
Rated power	150 kW
Rated speed	3600 r/min
Operating temperature	175℃
DC bus voltage	900 V
Pole-pairs number	4
Slot number	48

TABLE II
THE DESIGN VARIABLES

Symbol	Quantity	Min.	Max.
R_r	Inner radius of rotor	100 mm	150 mm
δ	Air-gap height	2 mm	10 mm
h_m	PMs height	5 mm	20 mm
h_s	Stator slot height	20 mm	50 mm
h_y	Stator yoke height	10 mm	40 mm
b_t	Stator teeth width	5 mm	20 mm
L_1	Core length	100 mm	300 mm
α_p	Pole-arc to pole-pitch ratio	0.5	1

S_f (Slot fill factor) $\leqslant$ 76%

0.5 T $\leqslant B_g$ (Air gap flux density) $\leqslant$ 0.8 T

1.3 T $\leqslant B_t$, B_y (Teeth and yoke flux density) $\leqslant$ 1.85 T

B. Implementation of MGA

Genetic algorithm (GA) is a stochastic, parallel evolutionary computation optimization method, which has been widely used for electromagnetic devices [3][9]. The standard GA may have some shortcomings such as prematurely, local optimal trap, and long time-consuming in solving the optimization of nonlinear complex problems, which using weighted coefficient method to solve the multi-objective optimization will meet the trouble of decision of the weighted coefficients in different objective functions, especially the objectives are not the same order of magnitude [3]. The proposed MGA can deal with multi objective problems in parallel. The MGA optimization combining with accurate SD model are shown in Fig. 4.

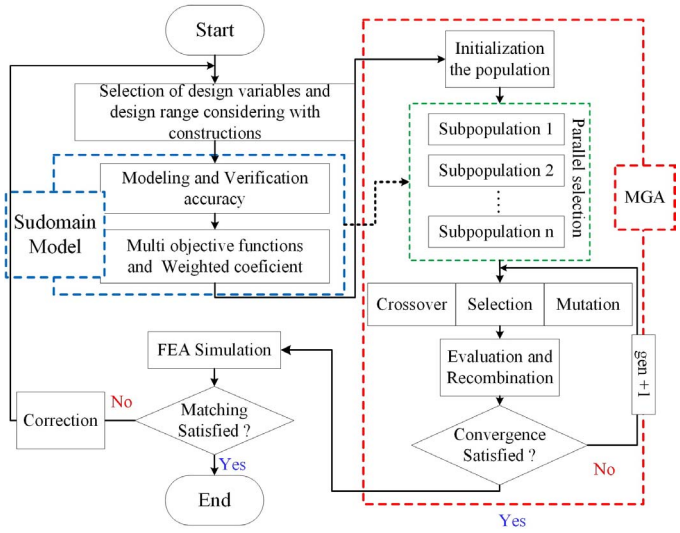

Fig. 4. Block diagram of MGA with SD model.

The conflict of feasible solution between the multi objective functions and constraints leads to the existence of Pareto set instead of the global optimum set in the process of optimization. In MGA, the parallel selection method is applied to solve the Pareto solution of multi objective problems. According to the significance of different objective functions, the corresponding individual number of sub-population will be determined. The details of parallel selection method as shown in Fig. 5.

The advantage of the parallel selection method is that each objective function can be independently performed in the corresponding sub-population, without considering about whether the weight coefficients of each object function are difficult to decide. In order to ensure the independence of subpopulation, the size of each subpopulation should be large enough.

The feasibility of the design is guaranteed by adding a penalty to the objective function due to constraint violations

$$F(X)=\begin{cases}\sum_{i=1}^{3} f_i(X) & X \text{ meet the constraints}\\ \sum_{i=1}^{3} f_i(X)\pm\sum_{j=1}^{6}\beta g_j(X) & X \text{ not meet the constraints}\end{cases} \quad (18)$$

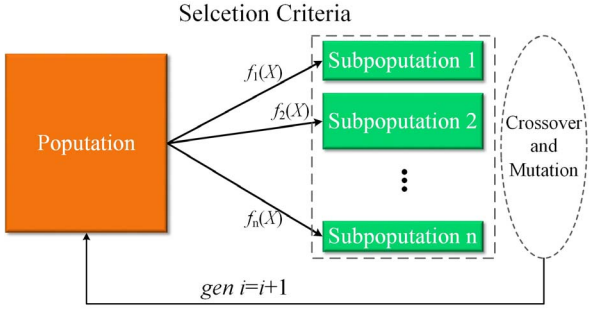

Fig. 5. Diagram of parallel selection method.

where g_j (X) is the constraint function, β is the penalty coefficient and the objective functions f_i (X) (i=1,2,3) are defined as follows

$$f_1(\mathrm{X})=(\sum_{i=3,5,7,...}^{15} B_i^{\,2})^{1/2} / B_1 \quad (19a)$$

$$f_2(\mathrm{X}) = P_{out} / (P_{Fe} + P_{Cu} + P_{mec} + P_{ad} + P_{out}) \quad (19b)$$

$$f_3(\mathrm{X}) = c_{Cu} M_{Cu} + c_{Fe} M_{Fe} + c_{PM} M_{PM} \quad (19c)$$

IV. Results

A. Optimal Design Results

Fig. 6 describe the evaluation of the optimal solution of the THD of air-gap flux density, efficiency and cost at the rated load during the optimization proceeding. The solutions of initial design, GA optimal design and MGA optimal design are shown in Table III.

In the process of optimization, it can be seen that the MGA optimization demonstrates better optimization capability and preferable convergence effect than the conventional GA optimization method.

TABLE III
THE SOLUTIONS OF TWO OPTIMIZATION METHODS

Symbol	Initial	GA	MGA
R_r	119 mm	100.1 mm	104.5 mm
δ	6 mm	6 mm	8.9 mm
h_m	6 mm	7.1 mm	9.5 mm
h_s	39 mm	36.4 mm	35.9 mm
h_y	15 mm	14.4 mm	12.2 mm
b_t	7.5 mm	6.3 mm	6.7 mm
L_1	160 mm	125.6 mm	115.8 mm
α_p	0.8	0.7065	0.6915

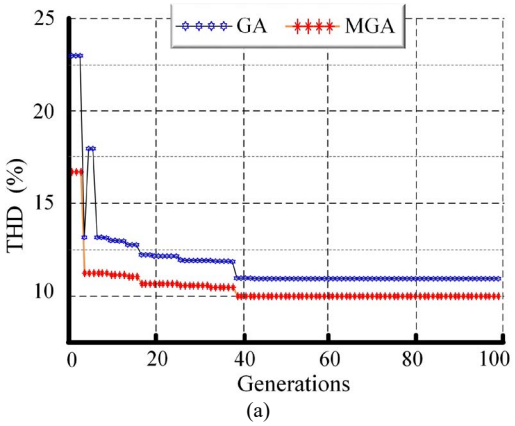

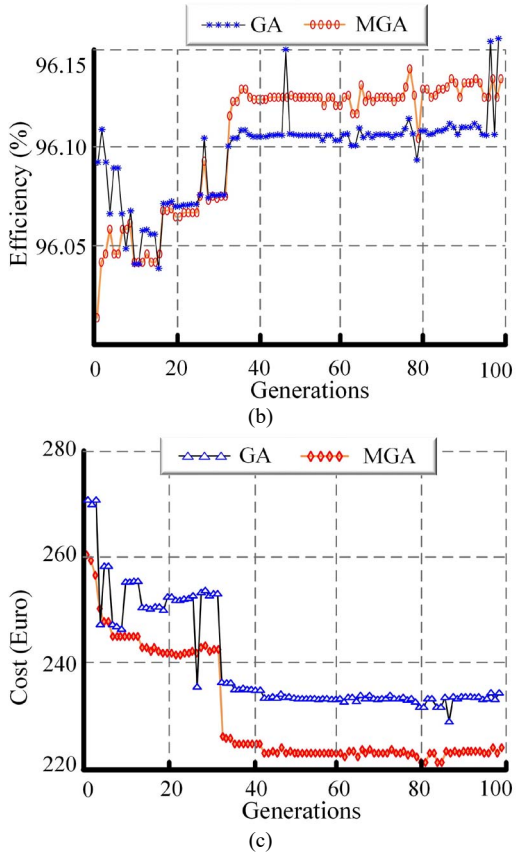

Fig. 6. The optimal solution variations of GA and MGA optimization method. (a) THD of air gap flux density (b) Efficiency under rated power (c) Total materials cost.

B. *Verification by FEA*

In order to verify the effectiveness of the improved GA optimization method, three types of simulation scheme of the 150kW-3600 r/min SPMSM are established. From the comparative results, the material cost is effectively decreased from 305.04 Euro to 235.6 Euro and down to 224.06. The load torque ripple validated by FEA is decreased from 1.41% to 0.67% and down to 0.65%, and the cogging torque is decreased from 2.96Nm to 0.41Nm and down to 0.26Nm.

Fig. 7 shows the comparative results of cogging torque by three types of design method.

Fig. 8 show the induced voltage waveforms and its fast Fourier transform (FFT) results of three design method.

The comparative results in Fig. 7 and Fig.8 verify the effectiveness of the spatial waveform optimization.

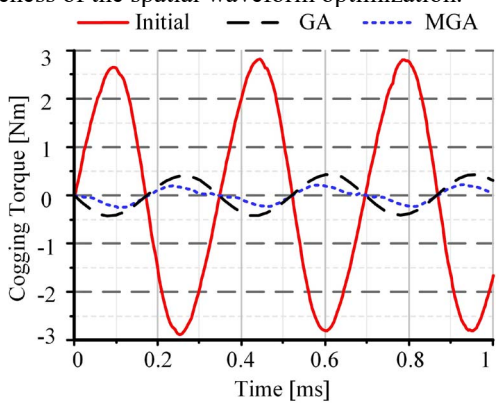

Fig. 7. Comparison of cogging torque

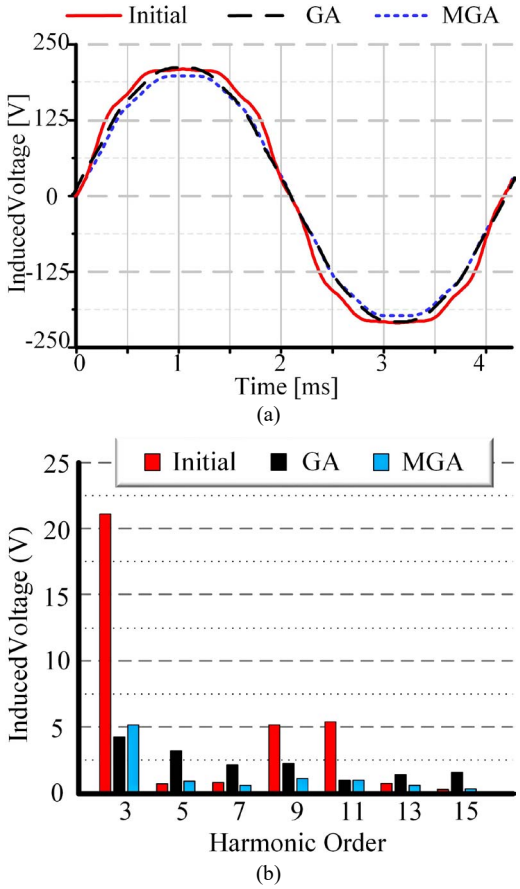

Fig. 8. Comparison of induced voltage (a) Waveforms. (b) Amplitude of the harmonics.

V. Conclusion

In this study, an improved genetic algorithm, as multi-independent-population genetic algorithm (MGA), is proposed, and combined with the accurate SD model to improve the multiple performance of SPMSM including the THD of flux density, efficiency and cost. Compared with the initial design and traditional GA optimal design, the application of MGA method to a 150-kw SPMSM brings the THD reduction of 5.68% and 1.08%, respectively; brings the cost reduction of 36.16% and 5.15% respectively; brings the efficiency enhancement of 0.02% and only reduction of 0.06%, respectively. Additionally, the effect of core saturation and heat load will be considered in further research.

References

[1] Shuhong Wang, and et al. "Multilevel Optimization for Surface Mounted PM Machine Incorporating With FEM, " *IEEE Trans. Magn.,* vol. 45, no. 10, pp. 4700-4703, Oct. 2009.

[2] Karthik Sindhya, and et al. "Design of a Permanent Magnet Synchronous Generator Using Interactive Multiobjective Optimization," *IEEE Trans. Ind. Electronic.* vol. 64, no. 12, pp. 9776-9783, Dec. 2017.

[3] Hui Li, Zhe Chen, and Henk Polinder, "Optimization of Multibrid Permanent-Magnet Wind Generator Systems," *IEEE Trans. Energy. Convers,* vol. 24, no. 1, pp. 82-92, Mar. 2009.

[4] Linh Dang, and et al. "Design Optimization with Flux Weakening of High-Speed PMSM for Electrical Vehicle Considering the Driving Cycle," *IEEE Trans. Ind. Electronic.* vol. 64, no. 12, pp. 9834-9843. Dec. 2017.

[5] Floran Martin, and et al. "Effect of Punching the Electrical Sheets on Optimal Design of a Permanent Magnet Synchronous Motor," *IEEE Trans. Magn.*, vol. pp, no. 99, pp. 1-4. 2017.

[6] Alireza Fatemi, and et al. "Large-Scale Design Optimization of PM Machines Over a Target Operating Cycle," *IEEE Trans. Ind. Applica.*, vol. 52, no. 5, pp. 3772-3782. Sept. 2016.

[7] Guodong Feng, Chunyan Lai, and Narayan C. Kar, "An Analytical Solution to Optimal Stator Current Design for PMSM Torque Ripple Minimization With Minimal Machine Losses," *IEEE Trans. Ind. Electronic.,* vol. 64, no. 10, pp. 7655-7665. Oct. 2017.

[8] Sisuda Chaithongsuk, and et al., "Optimal Design of Permanent Magnet Motors to Improve Field-Weakening Performances in Variable Speed Drives," *IEEE Trans. Ind. Electronic.,* vol. 59, no. 6, pp. 2484-2494. Jun. 2012.

[9] Tao Wang, Qingfeng Wang, "Optimization Design of a Permanent Magnet Synchronous Generator for a Potential Energy Recovery System," *IEEE Trans. Energy. Conver.*, vol. 27, no. 4, pp. 856-863, Dec. 2012.

[10] Jin Hwan Lee, and et. al., "Particle Swarm Optimization Algorithm With Intelligent Particle Number Control for Optimal Design of Electric Machines," *IEEE Trans. Ind. Electronic.*, vol. 65, no. 2, pp. 1791-1798. Feb. 2018.

[11] Pavel Ponomarev, and et. al., "Selection of Geometric Design Variables for Fine Numerical Optimizations of Electrical Machines," *IEEE Trans. Magn.,* vol 51, no. 12, 8114808, Dec. 2015.

[12] Jin Hwan Lee, and et al. "Distance-Based Intelligent Particle Swarm Optimization for Optimal Design of Permanent Magnet Synchronous Machine," *IEEE Trans. Magn.*, vol. 53, no. 6, 7206804, Jun. 2017.

[13] Chunyan Lai, and et al. "Investigations of the Influence of PMSM Parameter Variations in Optimal Stator Current Design for Torque Ripple Minimization," *IEEE Trans. Energy.*, Convers., vol. 32, no. 3, pp. 1052-1062, Sept. 2017.

[14] Lucian Nicolae Tutelea, and et al. "Line Start 1 Phase–Source Split Phase Capacitor Cage–PM Rotor–RelSyn Motor: Modeling, Performance, and Optimal Design With Experiments," *IEEE Trans. Ind. Electronic.*, vol. 65, no. 2, pp. 1772-1780. Feb. 2018.

[15] Kyung-Hun Shin, and et. al., "Analytical Calculation and Experimental Verification of Cogging Torque and Optimal Point in Permanent Magnet Synchronous Motors," *IEEE Trans. Magn.,* vol 53, no. 6, 8106204, Jun. 2017.

[16] Hong Guo, and et. al., "Robust design for the 9-slot 8-pole surfacemounted permanent magnet synchronous motor by analytical method-based multiobjectives particle swarm optimisation," *IET Electric Power Applications*, vol. 10, no. 2, pp. 117-124. 2016.

[17] Jian Gao, Guang Wang and et. al., "Cogging Torque Reduction by Elementary-Cogging-Unit Shift for Permanent Magnet Machines," *IEEE Trans. Magn.*, vol 53, no. 11, 8208705, Nov. 2017.

[18] Z. Q. Zhu, David Howe and C. C. Chan, "Improved Analytical Model for Predicting the Magnetic Field Distribution in Brushless Permanent-Magnet Machines, " *IEEE Trans. Magn.*, vol. 38, no. 1, pp. 229-238, Jan. 2002.

[19] Brandon N. Cassimere, Scott D. Sudhoff and Doug H. Sudhoff, "Analytical Design Model for Surface-Mounted Permanent-Magnet Synchronous Machines," *IEEE Trans. Energy. Convers*, vol. 24, no. 2, pp. 347-357, Jun. 2009.

[20] G. Bertotti, "General properties of power losses in soft ferromagnetic materials," *IEEE Trans. Magn.*, vol. 24, no. 1, pp. 621–630, Jan. 1988.

Jian Gao received the B.Eng., M.Eng. and Ph.D. degree from Hunan University, Changsha, China, in 2001,2004 and 2013, respectively.

From 2004 to 2017, he was a lecture of College of electrical and information engineering, Hunan University, and now he becomes an associate professor. His current research interests include permanent magnet machine system design and control.

Litao Dai received the B.S. degree in mathematics and applied mathematics from Harbin University of Commerce, Harbin, China, in 2015.

Since 2016, he was been a student with Hunan University, Changsha, China. His current research interests include permanent magnet machine electromagnetic analysis and optimal design.

Wenjuan Zhang received the B.Eng. and Ph.D. degree from Hunan University, Changsha, China, in 2007 and 2014, respectively.

Since 2014, she was a lecture of College of electronic information and electrical engineering, Changsha University, Changsha, China. Her current research interests include novel permanent magnet machine design and control.